Deterministic Models of an Active Magnetic Bearing System

Abdul Rashid Husain, Mohamad Noh Ahmad
Department of Mechatronics and Robotics,
Universiti Teknologi Malaysia, 81310, Skudai, Johor, Malaysia
Email: rashid@fke.utm.my, noh@fke.utm.my

Abdul Halim Mohd Yatim
Department of Energy Conversion,
Universiti Teknologi Malaysia, 81310, Skudai, Johor, Malaysia
Email: halim@ieee.org

Abstract— In this paper the development of mathematical model of voltage-input and current-input active magnetic bearing (AMB) system in deterministic form is presented. The AMB system, which is open-loop unstable and highly coupled due to nonlinearities inherited in the system such as gyroscopic effect and mass imbalance, requires a dynamic controller that can stabilize the system. In order to synthesize the controller, the nonlinear AMB model is transformed into its deterministic form by using the known upper and lower bounds of the parameters and the state variables of the system. The voltage-input AMB model shows that the system contains mismatched uncertainty and non-zero system states value which suggests that synthesizing nonlinear dynamic controller for this model is almost unfeasible. Overcoming these problems, the current-input AMB model, however, is in the structure that is more suitable for the design of a stabilizing controller. A result from a computer simulation work shows that the states of the system behave nonlinearly without feedback control; however, this final system model with its numerical values can be used for the design of a class of a dynamic controller for system stabilization.

Index Terms—Active Magnetic Bearing (AMB), determistic form, dynamic control, computer simulation

I. INTRODUCTION

An active magnetic bearing (AMB) system is a collection of electromagnets used to suspend an object and stabilization of the system is performed by feedback control. The system is composed of a floating mechanical rotor and electromagnetic coils that provide the controlled dynamic force and thus allowing the suspended object to move in its predefined functionality. Due to this non-contact operation, AMB system has many promising advantages for high-speed, high-temperature and clean-environment applications. Moreover, adjustable stiffness and damping characteristics also make the AMB suitable for elimination of vibration that presents in the system. Although the system is complex and considered an advance topic in term of its structural and control design, the advantages it offers outweigh the design complexity.

Application areas of magnetic bearings are still steadily expanding because of these practically useful features. A few of the AMB applications that receive huge attentions from many research groups around the globe are the flywheel energy and storage device [1][2], turbo molecular pump [3], compressor [4], Left Ventricle Assist Device (LVAD)[5] and artificial heart [6][7][8]. For the LVAD and artificial hearts applications particularly, the present of any debris or dust resulted from any mechanical contact is strictly intolerable since these particles can contaminate the circulating blood that definitely will cause more hazardous effects to human. The use of magnetic bearing, as opposed to the fluid film and mechanical bearings, has offered new opportunity in this application area in which constructing both of these devices that meet the very stringent requirement is a viable option.

A typical control block diagram of AMB system is as shown in Figure 1 where in order to stabilize the system, a position feedback of the rotor obtained from a few position sensors is required. The control algorithm that is designed to achieve the pre-specified performance of the system resides in the digital processor in the form of software code. Since AMB system requires a very fast response, Digital Signal Processing (DSP) based digital processor board is usually adapted as the main processor. The digital-to-analog converter (DAC) and the power amplifiers are the electronic circuits that convert the controlled signals to an appropriate level to the system. Other signal conditioning circuits such as noise filter and dc gain most of the time can be incorporated in the control algorithm or performed by additional circuit on the DSP board.

Magnetic bearing systems are designed in a few configurations to meet various specifications for different applications. In term of the rotor position, it can be oriented in horizontal or vertical position in which in latter configuration, the effect of gravity is uncoupled from system dynamics wherein the vertical displacement is controlled separately from the other set of magnetic coils controlling horizontal position [3][9]. The magnetic
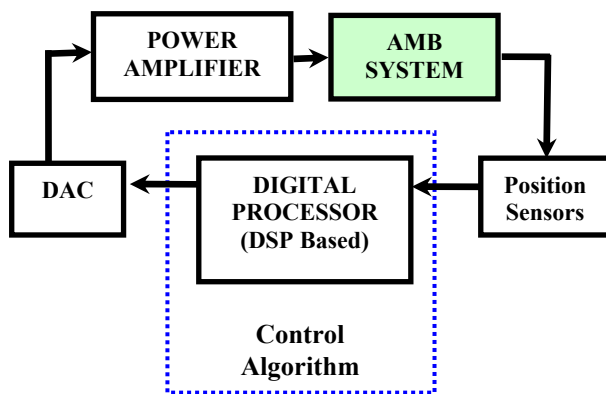
Figure 1. Block diagram of AMB control system

bearing system configuration with horizontal rotor orientation is however is more widely used as covered in majority of the references therein. Also, some of the applications such as the artificial heart, the rotor will be in both horizontal and vertical position due to its nature of operation which depends on the position and movement of the host [7] [8]. Other than the difference in rotor position, the designs of magnetic bearings that provide the dynamic force are also made in a few configurations. As shown in [10], the conical shape magnetic bearings are used where a small angle is introduced in the bearing design such that the dynamic forces produced by the complete set of the magnetic bearings are able to control both the radial and thrust motion. With this configuration, the number of magnetic bearings used is reduced; however, a more complicated control algorithm to stabilize the system is required due to the coupling effect of motion. An artificial intelligent based control algorithm for the system is covered in [11] however the model is linearized at an operating point such that the synthesis of the controller is feasible.

Another type of arrangement of the magnetic bearings is having three magnetic bearing at each end of the rotor which requires only six magnetic bearing in total for complete system [12]. However, the major trade-off in this configuration is the flux coupling effect between the bearings which requires a more complicated model to represent the nonlinear behavior of the system and further needs a more complicated stabilizing controller. In addition to this configuration, some systems have incorporated permanent magnets in the bearing which supply static forces to the system. The combination of this permanent magnets and active magnetic bearings form so-called hybrid magnetic bearings as have been highlighted in [1], [2], [8] and [13].

Another important aspect in magnetic bearing system is the method to stabilize and control the system to meet the need of the application. Both linear and nonlinear control laws have been covered in many research works and the choice of controllers usually relies on the structure of model established and the requirements of applications. Linear controllers are adapted more widely, however, nonlinear controllers promise more optimized power consumption which is favorable in most

applications [14][15]. For both of these types of controller families, the power amplifiers that supply the current to the system (or voltage) exist in three classes of mode of operation [16]. In Class-A power amplifier, the operation is performed such that a constant bias current is supplied all the magnetic coils where the value is set at the half of the allowable current value. The controlled currents are added to the bias current in one coil and subtracted from the bias current in the opposite coil that is in alignment to the direction of the force produced. This mode of operation is the most commonly used in magnetic bearing due to its good dynamic performance. For Class-B mode, a lower value of bias current is supplied to the magnetic coil but the controlled current is only added to only one side of the pair of magnetic bearing, according to the position of the rotor. Class-B mode, however, inherits poor bearing stiffness and poor robustness against system vibration which make it suitable for low performance applications. Then, when there is no bias current used, where only the controlled current is supplied to the magnetic bearing, it is categorized as Class-C power amplifier. In this mode, only nonlinear controllers work due to its singularity error at initial point of operation and severe nonlinearity that resulted when the control force is zero.

AMB system is considered an advance mechatronic system in which a successful design depends heavily on the mathematical models that represents the system behaviour at design stage [17]. The performance of the system can be accessed through computer simulation which is more cost effective and practical towards constructing the actual physical system. However, under these various AMB configurations, magnetic coils arrangement as well as different types of mode of power amplifiers, modeling the AMB system is in fact a very challenging task. Many of early works in AMB modeling involve the derivation of linear or linearized models which operate at certain operating condition. This procedure is performed in order to accommodate a linear dynamic controller for stabilization of the AMB system. The disadvantage of this approach is the model is valid at a very small operating condition and the system performance will degrade as the model of the physical system is perturbed from this operating point [18]. However, in order to maximize the performance of the system, the derived model needs to cover wider operational ranges that further forces the system into its nonlinear regime. In order to achieve this, a more sophisticated mathematical model that can describe the behaviour of the system within this boundary is required.

In this paper, two nonlinear mathematical models of a horizontal shaft AMB system are derived in which the gyroscopic effect and mass imbalance are also considered. The two AMB models are developed based on the system with voltages as the inputs and the system with currents as the inputs. The derived model will be presented in a state variable form that is suitable for the design of a class of robust controller. Figure 2 shows the five degree-of-freedom (DOF) horizontal AMB system that requires four pairs of electromagnetic coils to
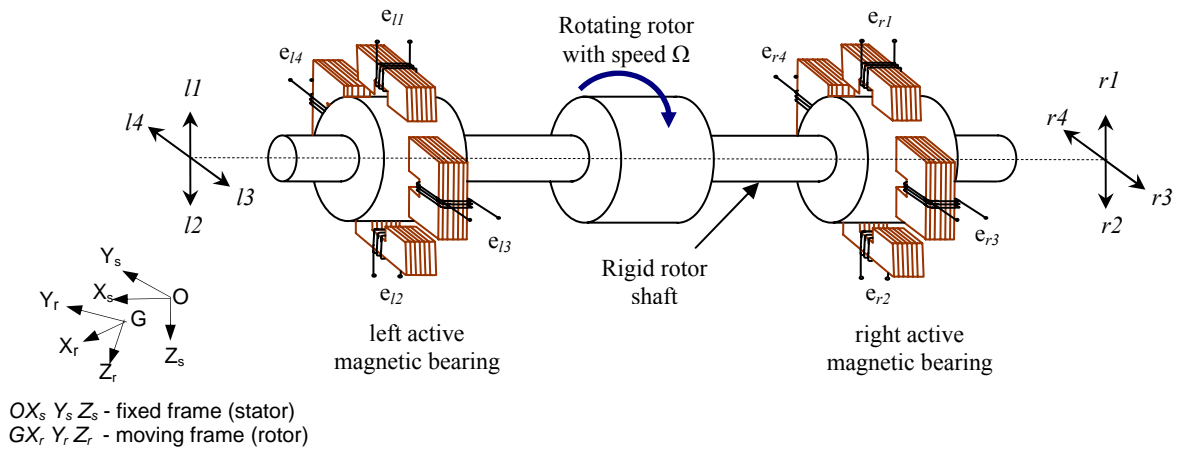
Figure 2. Cylindrical Horizontal Active Magnetic Bearing System

perform the radial control. The thrust control of the system is performed independently by another pair of electromagnetic coil and is not shown in the figure. The fifth DOF, which is the rotation around the x-axis, is supplied by external rotating machine in which the rotational speed is considered as a time-varying parameter. For the model with voltages as the input, eight voltage sources are supplied to the coils while for the model with current as inputs, similarly, the currents will be the inputs to the system.

This paper will be organized as follows: In section II, a review on the derivation of the equations of motion and the dynamic equation of electromagnetic coils will be performed based on [19] and [20]. In section III, for the both of the voltage-input and current-input AMB models, the integration of both sets of equations is carried out to form a state-space AMB model. The voltage-input model falls in the Class-A mode of operation while the current-input model belongs to Class-C mode. Then, in section IV, based on the upper and lower bounds of the system states and the rotational speed, both models are converted into their deterministic form where it can be shown that the voltage-input model contains system uncertainty and disturbance matrices which suffers mismatched condition. For the current-input model, the uncertainties present in the system, input and disturbance matrices, however, all of the uncertainties are in phase with the input channels but still the system is still highly nonlinear as portrayed in a simulation result. Finally, the conclusion in section V will summarize the work of this paper.

II. DYNAMIC EQUATIONS OF AMB SYSTEM

For the derivation of the mathematical model, cylindrical horizontal AMB system as shown in Figure 2 is used. Equations of motions of the rotor and the nonlinear electromagnetic coils equations are the two sets of equations that describe the dynamical behaviour of the system.

A. Equations of Motion

The equations of motion describe the dynamic movement of the rotor of the system. Assuming that the rotor is rigid floating body, the principle of flight dynamics is used to derive the equation. Based on the work in [19] and [20], the rotor's equations of motion for five DOF are

$$\ddot{y}_o = \frac{1}{m}[\alpha y_o + (f_{l3} - f_{l4} + f_{r4} - f_{r3}) + f_{dy}]$$

$$\ddot{z}_o = \frac{1}{m}[\alpha z_o + (f_{l2} - f_{l1} + f_{r2} - f_{r1}) + f_{dz} + mg]$$

$$\ddot{\theta} = \frac{-pJ_x}{J_y}\dot{\psi} + \frac{l}{J_y}((f_{l1} - f_{l2} + f_{r2} - f_{r1}) + f_{d\theta})$$

$$\ddot{\psi} = \frac{pJ_x}{J_y}\dot{\theta} + \frac{l}{J_y}((f_{l3} - f_{l4} + f_{r4} - f_{r3}) + f_{d\psi})$$

(1)

where m is the mass of the rotor, l is the longitudinal of length between the rotor mass centre to the electromagnetic coil, J_x is the moment of inertia around X_r, J_y is the moment around Y_r, α is the radial eccentricity coefficient, ψ and θ are angular displacement of rotor axis about Y_s and Z_s axes, y_o and z_o are the coordinates of rotor mass centre on Y_s and Z_s axes, f_{l1}, f_{l2}, f_{l3}, f_{l4}, f_{r1}, f_{r2}, f_{r3}, and f_{r4} are the nonlinear magnetic force produced by the bearings (stator) and exerted on the rotor, and f_{dy}, f_{dz}, $f_{d\psi}$ and $f_{d\theta}$ are terms for the imbalances that present in the system. It can be noticed from (1) that the imbalances act like external disturbances to the system which will cause the vibration to the rotor. The imbalance forces can be modeled as follows [21]

$$f_{dy} = m_o \varepsilon p^2 \cos(pt + \kappa)$$

$$f_{dz} = m_o \varepsilon p^2 \sin(pt + \kappa)$$

$$f_{d\theta} = \frac{(J_y - J_x)}{l} \tau p^2 \cos(pt + \lambda)$$

$$f_{d\psi} = \frac{(J_y - J_x)}{l} \tau p^2 \sin(pt + \lambda)$$

(2)

where m_o is the mass of unbalance, ε and τ are static and dynamic imbalances, κ and λ are initial phase values.

B. Electromagnetic Equations

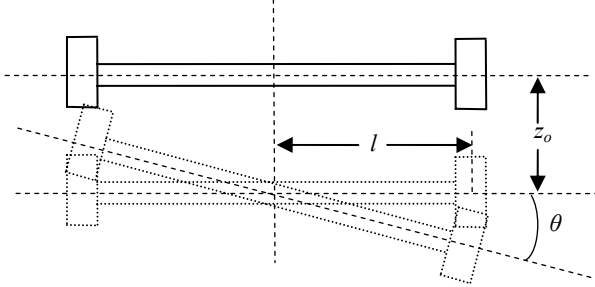There are two ways to model the dynamic of electromagnetic coils which are by using force-to-flux or

Figure 3. Cylindrical Horizontal Active Magnetic Bearing System

force-to-current relation. For this model, as claimed in [22], the force-to-flux relation for the dynamic coil is used due to the fact that both the force and flux depend inversely to the time varying airgap length which will give a better system performance under feedback control. The electromagnetic force f_j produced by jth electromagnetic coils is expressed in term of the airgap flux ϕ_j and the gap length g_j as shown below

$$f_j = k\phi_j^2\left(1+\frac{2g_j}{\pi h}\right) \quad,\quad j = l1, \cdots, l4, r1, \cdots, r4 \qquad (3)$$

where k is a constant and h is the width of the electromagnetic pole. The electric circuit equation that relates the airgap flux ϕ_j, the airgap length g_j and the input voltage e_j of the jth electromagnet is

$$e_j = N\frac{d\phi_j}{dt} + \frac{2R}{\mu_o AN}g_j\phi_j \quad,\quad j = l1, \cdots, l4, r1, \cdots, r4 \quad (4)$$

where N is the number of turn in each coil, R is the coil resistance, A is the area under one electromagnetic pole and $\mu_o = 4\pi \times 10^{-7}$ H/m is the permeability of free space. Notice that (4) is valid by assuming that the speed e.m.f and the leakage inductance produced by the coil are negligibly small.

C. Change of state variable – transformation matrix

From the control point of view, it is preferable to have the gap deviations as the state variables of the system instead of the coordinates of the mass center, yaw and pitch angles of the rotor. This is due to the fact that the gap deviations are easier to be measured than the rotor mass center either by using sensors or by designing observers [20]. The relation between the jth airgap of the electromagnetic coils and the rotor can be expressed as follows:

$$g_j = D_o + g_j' \quad,\quad j = l1, \cdots, l4, r1, \cdots, r4 \qquad (5)$$

where: D_o is the steady state gap length at equilibrium and g_j' is the gap length deviation from steady state value D_o.

Based on Figure 3 which shows the exaggerated view of the movement of the rotor in z-axis, assuming the angle θ is small such that $\sin\theta \approx \theta$, the relation between the airgaps in the AMB with rotor mass centre coordinate can be related as follows:

$$g = \begin{bmatrix} g_{l1}' \\ g_{r1}' \\ g_{l3}' \\ g_{r3}' \end{bmatrix} = - \begin{bmatrix} g_{l2}' \\ g_{r2}' \\ g_{l4}' \\ g_{r4}' \end{bmatrix} = \begin{bmatrix} (z_o - l\theta) \\ (z_o + l\theta) \\ (-y_o - l\psi) \\ (-y_o + l\psi) \end{bmatrix} \qquad (6)$$

With this equation a transformation matrix, T, can be established to perform the change the system variables.

$$T = \begin{bmatrix} 0 & 1 & -l & 0 \\ 0 & 1 & l & 0 \\ -1 & 0 & 0 & -l \\ -1 & 0 & 0 & l \end{bmatrix} \qquad (7)$$

III. AMB MODEL IN STATE-SPACE FORM

A. AMB Model with voltage input

Equations (1), (2), (3), (4) and (7) can now be easily integrated to form the model of horizontal AMB system in state-space form. Let the 16 state variables and 8 inputs of the system to be defined as follows:

$$\begin{aligned} x_1 &= g_{l1}' &,\quad x_2 &= g_{r1}' &,\quad x_3 &= g_{l3}' &,\quad x_4 &= g_{r3}' &,\\ x_5 &= \dot{x}_1 &,\quad x_6 &= \dot{x}_2 &,\quad x_7 &= \dot{x}_3 &,\quad x_8 &= \dot{x}_4 &,\\ x_9 &= \phi_{l1} &,\quad x_{10} &= \phi_{l2} &,\quad x_{11} &= \phi_{r1} &,\quad x_{12} &= \phi_{r2} &,\\ x_{13} &= \phi_{l3} &,\quad x_{14} &= \phi_{l4} &,\quad x_{15} &= \phi_{r3} &,\quad x_{16} &= \phi_{r4} &,\\ u_1 &= e_{l1} &,\quad u_2 &= e_{l2} &,\quad u_3 &= e_{r1} &,\quad u_4 &= e_{r2} &,\\ u_5 &= e_{l3} &,\quad u_6 &= e_{l4} &,\quad u_7 &= e_{r3} &,\quad u_8 &= e_{r4} &. \end{aligned}$$

Then, (8) below is the representation of the AMB system in state-space form.

$$\dot{\mathbf{x}}_v(t) = \mathbf{A}_v(\mathbf{x}_v, p, t)\mathbf{x}_v(t) + \mathbf{B}_v\mathbf{U}_v(t) + \mathbf{D}_v(p, t) \qquad (8)$$

It can be observed from this nonlinear model that the system matrix $\mathbf{A}_v(\mathbf{x}_v, p, t)$ is dependent to the state variables and the time-varying speed, p, while the disturbance matrix $\mathbf{D}_v(p, t)$ is only dependent on p. In order to facilitate the process to develop of dynamic controller, the equation above can be partitioned as shown below

$$\begin{bmatrix} \dot{\mathbf{x}}_{v1} \\ \dot{\mathbf{x}}_{v2} \\ \dot{\mathbf{x}}_{v3} \\ \dot{\mathbf{x}}_{v4} \end{bmatrix} = \begin{bmatrix} 0 & \mathbf{I} & 0 & 0 \\ \mathbf{A}_{v1} & \mathbf{A}_{v2} & \mathbf{A}_{v3} & \mathbf{A}_{v4} \\ 0 & 0 & \mathbf{A}_{v5} & 0 \\ 0 & 0 & 0 & \mathbf{A}_{v6} \end{bmatrix} \begin{bmatrix} \mathbf{x}_{v1} \\ \mathbf{x}_{v2} \\ \mathbf{x}_{v3} \\ \mathbf{x}_{v4} \end{bmatrix} + \begin{bmatrix} 0 & 0 \\ 0 & 0 \\ \mathbf{B}_{v1} & 0 \\ 0 & \mathbf{B}_{v2} \end{bmatrix} \mathbf{U}_v + \begin{bmatrix} 0 \\ \mathbf{D}_{v1} \\ 0 \\ 0 \end{bmatrix}$$

$$(9)$$

where: $\dot{\mathbf{x}}_{v1} = [g'_{l1}, g'_{r1}, g'_{l3}, g'_{r3}]$, $\dot{\mathbf{x}}_{v2} = [\dot{g}'_{l1}, \dot{g}'_{r1}, \dot{g}'_{l3}, \dot{g}'_{r3}]$, $\dot{\mathbf{x}}_{v3} = [\phi_{l1}, \phi_{l2}, \phi_{r1}, \phi_{r2}]$ and $\dot{\mathbf{x}}_{v4} = [\phi_{l1}, \phi_{l2}, \phi_{r1}, \phi_{r2}]$. The elements of the matrices are shown in the appendix.

B. AMB Model with current input

In this section, a current-input AMB system is developed where the equation that relates the flux and current is given in [11] as follows:

$$\phi_j = \left(\frac{\mu_o A_g N}{D_o + g_j} \right) i_j , \quad j = l1, \cdots, l4, r1, \cdots, r4 \qquad (10)$$

In this model, a bias current is introduced in the system such that the input current supplied to each coil is composed of the bias current and controller current. With the introduction of the bias current, the AMB now operates in Class A mode. The input currents are defined as follows:

$$i_{l1} = I_b + i_{cvl}, \; i_{l2} = I_b - i_{cvl} , \qquad (11a)$$

$$i_{r1} = I_b + i_{cvr}, \; i_{r2} = I_b - i_{cvr} , \qquad (11b)$$

$$i_{l3} = I_b + i_{chl}, \; i_{l4} = I_b - i_{chl} , \qquad (11c)$$

$$i_{r3} = I_b + i_{chr}, \; i_{r4} = I_b - i_{chr} , \qquad (11d)$$

where: I_b is the bias current, i_{cvl} is the controlled current of the *l1-l2* magnetic bearing pair, i_{cvr} is the controlled current of the *r1-r2* magnetic bearing pair, i_{chl} is the controlled current of the *l3-l4* magnetic bearing pair and i_{chr} is the controlled current of the *r3-r4* magnetic bearing pair. Repeating the process in previous model, equations (1), (2), (3) ,(7), (10) and (11) are rearranged to form the current-input AMB model as shown by (12) and (13) below,

$$\dot{\mathbf{x}}_c(t) = \mathbf{A}_c(p,t)\mathbf{x}_c(t) + \mathbf{B}_c(\mathbf{x}_c,\mathbf{U},t)\mathbf{U}_c(t) + \mathbf{D}_c(\mathbf{x}_c,p,t)$$
$$(12)$$

$$\begin{bmatrix} \dot{\mathbf{x}}_{c1} \\ \dot{\mathbf{x}}_{c2} \end{bmatrix} = \begin{bmatrix} 0_{4\times4} & \mathbf{I}_{4\times4} \\ \mathbf{A}_{c1} & \mathbf{A}_{c2} \end{bmatrix} \begin{bmatrix} \mathbf{x}_{c1} \\ \mathbf{x}_{c2} \end{bmatrix} + \begin{bmatrix} 0 \\ \mathbf{B}_{c1} \end{bmatrix} \mathbf{U} + \begin{bmatrix} 0 \\ \mathbf{D}_{c1} \end{bmatrix} \qquad (13)$$

where: $\mathbf{x}_{c1} = \mathbf{x}_{v1}$ and $\mathbf{x}_{c2} = \mathbf{x}_{v2}$. The elements of the matrices are not shown in this paper since it can be derived quite easily based by following the method used for voltage-input model. There are a few major differences between voltage-input and current-input AMB models developed above. The most obvious one is the number of state variables in current-input model is reduced to only eight state variables which is only half of the states in voltage-input model. This is due to the fact that the coil voltage relation (4) is not included in the development of the current-input model. The other differences are the system matrix, input matrix, as well as the disturbance vector and these differences are tabulated in Table 2 which highlights the variables of each of these matrices and vector. These have resulted different upper and lower bound values of the matrices which further changes the values of the uncertainty and disturbances

needed for the controller development. The procedure will be more apparent in as explained in the next section.

TABLE I.
MATRICES FOR BOTH AMB MODELS

Voltage-input AMB Model	Current Input AMB Model
$\mathbf{A}_v(\mathbf{x}_v, p, t)$	$\mathbf{A}_c(p, t)$
$\mathbf{B}$	$\mathbf{B}_c(\mathbf{x}_v, \mathbf{U}, t)$
$\mathbf{D}_v(p,t)$	$\mathbf{D}_c(\mathbf{x}_v, p, t)$

V. AMB MODEL AS UNCERTAIN SYSTEM

A. Voltage-input AMB model

In order to synthesize a type of robust controller for this class of system, the AMB model derived in previous section will be treated as uncertain system in which deterministic approach to classify the system will be used based on [23]. By using this approach, the AMB model can be decomposed into its nominal and uncertain parts as shown below

$$\mathbf{x}_v(t) = [\mathbf{A}_v + \Delta\mathbf{A}_v(\mathbf{x}_v, p, t)]\mathbf{x}_v(t) + \mathbf{B}_v\mathbf{U}_v(t) + \mathbf{D}_v(p,t)$$
$$\mathbf{y}_v(t) = \mathbf{C}_v\mathbf{x}_v(t)$$
$$(14)$$

where $\Delta\mathbf{A}_v(\mathbf{x}_v,p,t)$ represents the uncertainty of the system matrix and $\mathbf{D}_v(p,t)$ is the disturbance matrix associated with speed dependent of imbalance. $\mathbf{A}_v$ and $\mathbf{B}_v$ are the nominal constant matrices of the system. The decomposition into this deterministic form is possible due to the fact that the all the maximum and minimum values of state variables and rotor speed are known. The elements of the $\Delta\mathbf{A}_v(\mathbf{x}_v,p,t)$ and $\mathbf{D}_v(p,t)$ system and disturbance matrices, respectively, can be calculated based on these available bounds. The minimum and maximum bounds of all the state variables and the rotor speed are as follows:

$$-0.55 \, mm \le x_i \le 0.55 \, mm , \; \text{for } i = 1,2,3,4, \qquad (15a)$$

$$0 \, m \; \le x_i \le 1.87 \, m/sec , \; \text{for } i = 5,6,7,8, \qquad (15b)$$

$$0 \, Wb \le x_i \; \le 10.0 \times 10^{-4} \, Wb , \; \text{for } i = 9, \ldots, 16, \qquad (15c)$$

and

$$0 \, rad/sec \le p \le 3142 \, rad/sec . \qquad (15d)$$

Then, by using these values and the other system parameter values as shown in Table II, each element of the system and disturbance matrices can be calculated and specified in the following form:

$$\underline{a}_{ij} \le a_{ij}(x_v, p, t) \le \overline{a}_{ij} \qquad (16a)$$

$$\underline{d}_j \le d_j(p, t) \le \overline{d}_j \qquad (16b)$$

for $i = 1, \ldots, 16$, and $j = 1, \ldots, 16$, where $a_{ij}(x_v,p,t)$ and $d_j(p,t)$ are the element of $\mathbf{A}_v(\mathbf{x}_v,p,t)$ and $\mathbf{D}_v(p,t)$ matrices respectively. The upper and lower bars indicate the

maximum and minimum values of the elements. Since these bounds are known, the system matrix can be written in the following form:

$$\mathbf{A}_v(\mathbf{x}_v, p, t) = \mathbf{A}_v + \Delta\mathbf{A}_v(\mathbf{x}_v, p, t) \qquad (17)$$

For this class of AMB system model, it can be noticed that for the disturbance matrix, $\mathbf{D}_v(p,t)$, only the maximum value of the elements are needed since these values represent the highest disturbance values caused by the imbalance which should be eliminated from the system. By using the values of the bounds given by (15), and the deterministic form of system matrix given by (14), the nominal and uncertain values of system matrix, a well as the values of disturbance matrix are calculated and given in the appendix. The norm for these matrices can also be calculated and the values are as follows:

$$\|\Delta\mathbf{A}_v\| = 5.6003 \times 10^4 \quad, \quad \|\mathbf{D}_v\| = 1.5595 \times 10^3 \quad. \qquad (18)$$

From the structure of the matrices, it can be shown that both the uncertainty and disturbance matrices suffer mismatched condition which means that the elements of the uncertainty and disturbance matrices do not lie in the range space of the input matrix $\mathbf{B}_v$. Also, the mismatched condition can be checked by using the rank test as shown below in which the results agree with the aforementioned mismatched condition.

$$\text{rank}[\mathbf{B}_v] \neq \text{rank}\,[\mathbf{B}_v, \Delta\mathbf{A}_v(\mathbf{x}_v,p,t)],$$
$$\text{rank}[\mathbf{B}_v] \neq \text{rank}\,[\mathbf{B}_v, \mathbf{D}_v(p,t)]. \qquad (19)$$

By having this mismatched condition, the input voltages of the system do not have direct access to the mismatched elements. Thus, this has made the design of the robust controller that can eliminate the disturbance and to achieve robustness towards system uncertainty a challenging task. Another difficulty arise from this model is the selection of the states of the system in which the fluxes (synonymously the current) of the electromagnetic coils selected as the states need to converge to zero to achieve system stability. However, this is impractical since as the fluxes go to zero, the input to the rotor is zero and no control occurs in the system. Both of these difficulties, however, are alleviated in the current-input model and make it suitable for development of dynamic controller.

B. Current-input AMB model

By following the method in the previous section, the deterministic model for current-input AMB system is shown by (15),

$$\mathbf{x}_c(t) = [\mathbf{A}_c + \Delta\mathbf{A}_c(p,t)]\mathbf{x}_c(t) + [\mathbf{B}_c + \Delta\mathbf{B}_c(\mathbf{x}_c, p, t)]\mathbf{U}_c(t)$$
$$+ \Delta\mathbf{D}_c(\mathbf{x}_c, p, t)$$
$$\mathbf{y}_c(t) = \mathbf{C}\mathbf{x}_c(t) \qquad (20)$$

and the nominal and uncertain system and input matrices can be represented by (20) and (21) as follows:

$$\mathbf{A}_c(p,t) = \mathbf{A}_c + \Delta\mathbf{A}_c(p,t) \qquad (21)$$

TABLE II.
PARAMETER FOR HORIZONTAL AMB SYSTEM [20][21]

Symbol	Parameter	Value [Unit]
m	Mass of Rotor	1.39×10^1 [kg]
A_g	Area of coil	1.532×10^{-3} [m^2]
J_x	Moment of Inertia about X	1.34×10^{-2} [kg.m^2]
J_y	Moment of Inertia about X	2.32×10^{-1} [kg.m^2]
D_o	Steady airgap	5.50×10^{-4} [m]
R	Coil Resistance	1.07×10 [Ω]
L	Coil Inductance	2.85×10^{-1} [H]
I_b	Bias Current	2.0 [A]
l	Distance between Mass centre to coil	1.30×10^{-1} [m]
α	Rotor radial eccentricity coefficient	1.0 [N/m]
μ_o	Permeability of free space	$4\pi \times 10^{-7}$ [H/m]
N	Number of Turn	400 [Turn]
h	Pole Width	0.04 [m]
k	Proportional Constant	4.6755576×10^8 [N/Wb^2]
ε	Static imbalance	1.0×10^{-4} [m]
τ	Dynamic imbalance	4.0×10^{-4} [rad]

$$\mathbf{B}_c(\mathbf{x}_c, p, t) = \mathbf{B}_c + \Delta\mathbf{B}_c(\mathbf{x}_c, p, t) \qquad (22)$$

Again, by using the range of operations of the states and rotor speed as given by (11), the upper and lower bounds of all the elements of the system, input and disturbance matrices can be calculated and lie in the following range of values,

$$\underline{a}_{ij} \leq a_{ij}(p,t) \leq \overline{a}_{ij} \qquad (23a)$$

$$\underline{b}_{ij} \leq b_{ij}(\mathbf{x}_c, p, t) \leq \overline{b}_{ij} \qquad (24b)$$

$$\underline{d}_j \leq d_j(\mathbf{x}_c, p, t) \leq \overline{d}_j \qquad (25c)$$

for $i = 1, \ldots, 8$ and $j = 1, \ldots, 8$, where $a_{ij}(p,t)$, $b_{ij}(\mathbf{x}_c,p,t)$ and $d_j(\mathbf{x}_c,p,t)$ are the element of $\mathbf{A}_c(p,t)$, $\mathbf{B}_c(\mathbf{x}_v,p,t)$ and $\mathbf{D}_c(p,t)$ matrices respectively. Thus, the norm value of the uncertainties using these values can be obtained as follows:

$$\left.\begin{array}{l} \|\Delta\mathbf{A}_c\| = 90.7443 \ , \\ \|\Delta\mathbf{B}_c\| = 244.9987 \ , \\ \|\mathbf{D}_c\| = 2.313 \times 10^3 \ . \end{array}\right\} \qquad (26)$$

With these values of the norm bounded uncertainties, the deterministic model of the AMB system with current input is complete and a class of robust controller can be developed. As opposed to voltage-input AMB model (8), the current-input model (12) is in the structure where all the uncertainties are matched and the states are selected
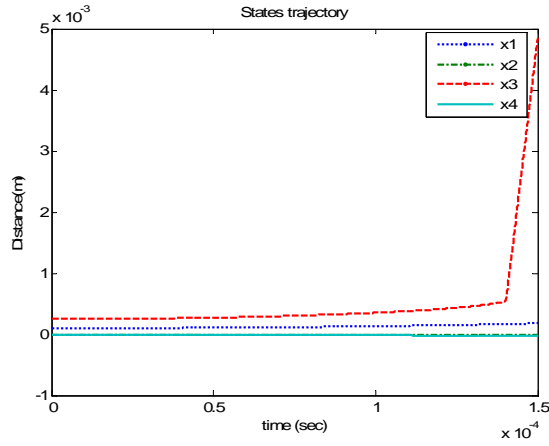
Figure 4. Trajectory of the states of the system under no control effort

such that the states will converge to zero when the system meets its stability condition. These two conditions definitely offer more flexibility in the design of the dynamic controller. To portray the nonlinearity in the system, the AMB model (12) is simulated by using MATLAB® and Simulink®, and the trajectory of the states of the system is shown in Figure 4. With initial conditions of the states $[x_1\ x_2\ x_3\ x_4]^T = [1.0 \times 10^{-4}\ 0.0\ 2.5 \times 10^{-4}\ 0.0]^T$ *m*, all of the states rapidly diverge from zero (equilibrium point) and this condition highlight the need of the dynamic controller to stabilize the system. Controllers in the family of Sliding Mode Control as theoretically developed in [24][25] and [26] are to appear suitably practicable for this AMB system due to its robustness and reliable performance in application into nonlinear system. The development and the implementation of the controller that can stabilize the system as well to achieve some system requirement will be the next milestone of this work.

V. CONCLUSION

In this work, the nonlinear mathematical models of AMB system based on both the voltage-input and current-input model have been developed. The nonlinear models are transformed into deterministic form in which the numerical values of all of the uncertainties that present are obtained. The norms of the uncertainties are also calculated in which the values represent the bounded values of the nonlinearities in the system. The models produced are arranged in a class of system that allows an appropriate structure of dynamic controller to be synthesized to stabilize and to meet the requirement of system performance. The development of the controller will be the future direction of this work and a suggestion of application of SMC is also highlighted.

APPENDIX A THE ELEMENTS OF VOLTAGE-INPUT AMB MODEL

$$\mathbf{A}_1 = \begin{bmatrix} a_1^{11} & a_1^{12} & 0 & 0 \\ a_1^{21} & a_1^{22} & 0 & 0 \\ \hdashline 0 & 0 & a_1^{33} & a_1^{34} \\ 0 & 0 & a_1^{43} & a_1^{44} \end{bmatrix}, \quad \mathbf{A}_2 = \begin{bmatrix} 0 & 0 & a_2^{13} & a_2^{14} \\ 0 & 0 & a_2^{23} & a_2^{24} \\ \hdashline a_2^{31} & a_2^{32} & 0 & 0 \\ a_2^{41} & a_2^{42} & 0 & 0 \end{bmatrix},$$

$$\mathbf{A}_3 = \begin{bmatrix} a_3^{11} & a_3^{12} & a_3^{13} & a_3^{14} \\ a_3^{21} & a_3^{22} & a_3^{23} & a_3^{24} \\ \hdashline 0 & 0 & 0 & 0 \\ 0 & 0 & 0 & 0 \end{bmatrix}, \quad \mathbf{A}_4 = \begin{bmatrix} 0 & 0 & 0 & 0 \\ 0 & 0 & 0 & 0 \\ \hdashline a_4^{31} & a_4^{32} & a_4^{33} & a_4^{34} \\ a_4^{41} & a_4^{42} & a_4^{43} & a_4^{44} \end{bmatrix},$$

$$\mathbf{A}_5 = \begin{bmatrix} a_5^{11} & 0 & 0 & 0 \\ 0 & a_5^{22} & 0 & 0 \\ \hdashline 0 & 0 & a_5^{33} & 0 \\ 0 & 0 & 0 & a_5^{44} \end{bmatrix}, \quad \mathbf{A}_6 = \begin{bmatrix} a_6^{11} & 0 & 0 & 0 \\ 0 & a_6^{22} & 0 & 0 \\ \hdashline 0 & 0 & a_6^{33} & 0 \\ 0 & 0 & 0 & a_6^{44} \end{bmatrix},$$

$$\mathbf{B}_1 = \begin{bmatrix} b_1^{11} & 0 & 0 & 0 \\ 0 & b_1^{22} & 0 & 0 \\ \hdashline 0 & 0 & b_1^{33} & 0 \\ 0 & 0 & 0 & b_1^{44} \end{bmatrix}, \quad \mathbf{B}_2 = \begin{bmatrix} b_2^{11} & 0 & 0 & 0 \\ 0 & b_2^{22} & 0 & 0 \\ \hdashline 0 & 0 & b_2^{33} & 0 \\ 0 & 0 & 0 & b_2^{44} \end{bmatrix},$$

$$\mathbf{D}_1 = \begin{bmatrix} \left(g + \dfrac{m_o}{m}\varepsilon p^2 \sin(pt) - \left(\dfrac{J_y - J_x}{J_y}\right)l\tau p^2 \cos(pt)\right) \\ \left(g + \dfrac{m_o}{m}\varepsilon p^2 \sin(pt) + \left(\dfrac{J_y - J_x}{J_y}\right)l\tau p^2 \cos(pt)\right) \\ -\left(\dfrac{m_o}{m}\varepsilon p^2 \cos(pt) + \left(\dfrac{J_y - J_x}{J_y}\right)l\tau p^2 \sin(pt)\right) \\ -\left(\dfrac{m_o}{m}\varepsilon p^2 \cos(pt) - \left(\dfrac{J_y - J_x}{J_y}\right)l\tau p^2 \sin(pt)\right) \end{bmatrix},$$

$$a_1^{11} = a_1^{12} = a_1^{21} = a_1^{22} = a_1^{33} = a_1^{34} = a_1^{43} = a_1^{44} = \frac{\alpha}{2m},$$

$$a_2^{13} = a_2^{24} = a_2^{32} = a_2^{41} = -\frac{pJ_y}{2J_x},$$

$$a_2^{14} = a_2^{23} = a_2^{31} = a_2^{42} = \frac{pJ_y}{2J_x}$$

$$a_3^{11} = -H_1 k\left(1 + \frac{2(D_o + x_1)}{\pi h}\right)x_9, \quad a_3^{12} = H_1 k\left(1 + \frac{2(D_o - x_1)}{\pi h}\right)x_{10},$$

$$a_3^{13} = H_2 k\left(1 + \frac{2(D_o + x_2)}{\pi h}\right)x_{11}, \quad a_3^{14} = -H_2 k\left(1 + \frac{2(D_o - x_2)}{\pi h}\right)x_{12},$$

$$a_3^{21} = H_2 k\left(1 + \frac{2(D_o + x_1)}{\pi h}\right)x_9, \quad a_3^{22} = -H_2 k\left(1 + \frac{2(D_o - x_1)}{\pi h}\right)x_{10},$$

$$a_3^{23} = -H_1 k\left(1 + \frac{2(D_o + x_2)}{\pi h}\right)x_{11}, \quad a_3^{24} = H_1 k\left(1 + \frac{2(D_o - x_2)}{\pi h}\right)x_{12},$$

$$a_4^{31} = -H_1 k\left(1 + \frac{2(D_o + x_3)}{\pi h}\right)x_{13}, \quad a_4^{32} = H_1 k\left(1 + \frac{2(D_o - x_3)}{\pi h}\right)x_{14},$$

$$a_4^{33} = H_2 k\left(1 + \frac{2(D_o + x_4)}{\pi h}\right)x_{15}, \quad a_4^{34} = -H_2 k\left(1 + \frac{2(D_o - x_4)}{\pi h}\right)x_{16},$$

$$a_4^{41} = H_2 k \left(1 + \frac{2(D_o + x_3)}{\pi h}\right) x_{13}, \; a_4^{42} = -H_2 k \left(1 + \frac{2(D_o - x_3)}{\pi h}\right) x_{14},$$

$$a_4^{43} = -H_1 k \left(1 + \frac{2(D_o + x_4)}{\pi h}\right) x_{15}, \; a_4^{44} = H_1 k \left(1 + \frac{2(D_o - x_4)}{\pi h}\right) x_{16},$$

$$a_5^{11} = -q(D_o + x_4)x_9, \; a_5^{22} = -q(D_o - x_1)x_{10},$$

$$a_5^{33} = -q(D_o + x_2)x_{11}, \; a_5^{44} = -q(D_o - x_2)x_{11},$$

$$a_6^{11} = -q(D_o + x_3)x_{12}, \; a_6^{22} = -q(D_o - x_3)x_{13},$$

$$a_6^{33} = -q(D_o + x_4)x_{15}, \; a_6^{44} = -q(D_o - x_4)x_{16},$$

$$b_1^{11} = b_1^{22} = b_1^{33} = b_1^{44} = b_2^{11} = b_2^{22} = b_2^{33} = b_2^{44} = \frac{1}{N}$$

$$\Delta \mathbf{A}_2 = 10^4 \begin{bmatrix} 0 & 0 & 1.355 & 1.355 \\ 0 & 0 & 1.355 & 1.355 \\ \hline 1.355 & 1.355 & 0 & 0 \\ 1.355 & 1.355 & 0 & 0 \end{bmatrix},$$

$$\Delta \mathbf{A}_3 = 10^4 \begin{bmatrix} 3.4441 & 3.441 & 0.0215 & 0.0215 \\ 0.0215 & 0.0215 & 3.4441 & 3.4441 \\ \hline 0 & 0 & 0 & 0 \\ 0 & 0 & 0 & 0 \end{bmatrix},$$

$$\Delta \mathbf{A}_4 = 10^4 \begin{bmatrix} 0 & 0 & 0 & 0 \\ 0 & 0 & 0 & 0 \\ \hline 3.4441 & 3.4441 & 0.0215 & 0.0215 \\ 0.0215 & 0.0215 & 3.4441 & 3.4441 \end{bmatrix},$$

$$\Delta \mathbf{A}_5 = \Delta \mathbf{A}_6 = \begin{bmatrix} 38.216 & 0 & 0 & 0 \\ 0 & 38.216 & 0 & 0 \\ \hline 0 & 0 & 38.216 & 0 \\ 0 & 0 & 0 & 38.216 \end{bmatrix},$$

$$\mathbf{D}_1 = \begin{bmatrix} -43.204 \\ 844.676 \\ -1097.956 \\ -714.944 \end{bmatrix}.$$

REFERENCES

[1] S. C. Mukhopadhyay, T. Ohji, M. Iwahara, and S. Yamada, " Modeling and Control of a New Horizontal-Shaft Hybrid-Type Magnetic Bearing ," *IEEE Trans. On Ind. Elec.*, vol. 47, no. 1, pp. 100–108, Feb. 2000.

[2] M. Komori, M. Kumamoto, and H. Kobayashi, "A Hybrid-Type Superconducting Magnetic Bearing System with Nonlinear Control," *IEEE Trans. on Applied Superconductivity*, vol. 8, no.2, pp. 79–83, June 1998.

[3] S. Sivrioglu and K. Nonami, " Sliding Mode Control With Time-Varying Hyperplane for AMB Systems," *IEEE/ASME Trans. on Mechatronics*, vol. 3(1), pp. 51-59, Mar. 1998.

[4] F. Losch, C. Gahler, and R. Herzog, "Low Order μ-Synthesis Controller Design for a Large Boiler Feed Pump Equipped with Active Magnetic Bearing," in *Proc. of IEEE Int. Conf. on Contr. Appl.*, August 1999, pp. 564–569.

[5] R. Schoeb, N. Barletta, A. Fleischli, G. Foiera, T. Gempp, H. G. Reiter, *et. al.*, "A Bearingless Motor For A Left Ventricular Assist Device (LVAD)," Proc. *In 7th Int. Symp. On Mag. Bearings*, Zurich Switzerland, Aug. 23-25, 2000.

[6] E. M. Maslen, G. B. Bearnson, P. E. Allaire, R. D. Flack, M. Baloh, E. Hilton, *et. al.*, "Feedback Control Applications in Artificial Hearts," *IEEE Control Sys. Mag.*, vol. 18, no. 6, pp. 26–34, Dec. 1998.

[7] J. H. Lee, P. E. Allaire, G. Tao, J. Decker, and X. Zhang, "Experimental Study of Sliding Mode Control for a Benchmark Magnetic Bearing System and Artificial Heart Pump Suspension', *IEEE Trans. on Contr. Sys. Tech.*, vol. 11, no. 1, pp. 128–138, Jan. 2003.

[8] J. X. Shen, K. J. Tseng, D. M. Vilathgamuwa and W. K. Chan, "A Novel Compact PMSM with Magnetic Bearing for Artificial Heart Application," *IEEE Trans. On Ind. Elec.*, vol. 36, no. 4, pp. 1061–1068, July/August 2000.

[9] A. F. Mohamed and I.B. Vishniac, "Imbalance Compensation and Automatic Balancing in Magnetic Bearing Systems Using the Q-Parameterization Theory", *IEEE Trans. on Contr. Sys. Tech.*, vol.3, no.2, pp. 202–221, June 1995.

[10] A. M. Mohamed and F. P. Emad," Conical Magnetic Bearings with Radial and Thrust Control," *IEEE Trans. on Auto Control*, vol. 37, no. 12, pp. 1859–1868, Dec 1992.

[11] S. J. Huang and L. C. Lin, "Fuzzy Dynamic Output Feedback Control With Adaptive Rotor Imbalance Compensation for Magnetic Bearing Systems," *IEEE Trans. on Sys., Man and Cybernatics – PART B: Cybern.*, vol. 37, no. 4, pp. 1854–1864, August 2004.

[12] C. T. Hsu and S. L. Chen, "Nonlinear control of a 3-pole active magnetic bearing system," *Automatica* 39, pp. 291–298, 2003.

[13] H. Kanebako and Y. Okada, " New Design of Hybrid-Type Self-Bearing Motor for Small, High-Speed Spindle," *IEEE/ASME Trans. on Mechatronics*, vol. 8, no. 1, pp. 111-119, Mar. 2003.

[14] J. Levine, J. Lottin and J. C. Ponsart, "A Nonlinear Approach to the Control of Magnetic Bearings," *IEEE Trans. on Contr. Sys. Tech.*, vol.4, no.5, pp. 524–544, Sept. 1996.

[15] A. Charara, J. De Miras and B. Caron, "Nonlinear Control of a Magnetic Levitation System Without Premagnetization," *IEEE Trans. on Contr. Sys. Tech.*, vol.4, no.5, pp. 513–523, Sept. 1996.

[16] M. N. Sahinkaya and A. E. Hartavi, "Variable Bias Current in Magnetic Bearings for Energy Optimization"

IEEE Trans. on Magnetics, vol. 43, no. 3, pp. 1052-1060, March 2007.

[17] N. Steinschaden, and H. Ecker, "A Nonlinear Model for Radial Magnetic Bearings," in *Proc. of 3rd Matnmod, 3rd IMACS Symp. Of Math. Modeling*, Vienna, Austria, Feb. 2-4, 2000.

[18] J. D. Lindlau and C. R. Knospe, "Feedback Linearization of an Active Magnetic Bearing With Voltage Control," *IEEE Trans. On Cont. Sys. Tech.*, vol. 10, no. 1, pp. 79–83, Jan. 2002.

[19] A. R. Husain, M. N. Ahmad, and A. H. Mohd Yatim, "Modeling of A Nonlinear Conical Active Magnetic Bearing System with Rotor Imbalance and Speed Emf," *Int. Conf. in Man-Machines Systems(ICoMMS)*, Langkawi, Malaysia, Sept 15-16, 2006.

[20] F. Matsumura, and T. Yoshimoto, "System modeling and control design of a horizontal shaft magnetic bearing system," *IEEE Trans. Magnetics*, vol MAG-22, no. 3, pp. 196-203, May 1986.

[21] A. M. Mohamed, I. M. Hassan, A. M. K. Hashem, "Elimination of Imbalance Vibrations in Magnetic bearing System Using Discrete-Time Gain-Scheduled Q-Parameterization Controllers," in *Proc. Of IEEE Conf. Int, Conf. on Contr Application*, August 1999, pp. 737-742.

[22] A. M. Mohamed and F. P. Emad, "Comparison between Current and Flux Control in Magnetic Bearing Systems," in *Proceedings. of the American Control Conference*, June 1993, pp. 2356-2362.

[23] J. H. S. Osman and P. D. Roberts, "Two Level Control Strategy for Robot Manipulators," *Int. Journal of Control*, vol. 61, no. 6, pp. 1201 – 1222, June 1995.

[24] G. Wheeler, C, Y. Sun and Y. Stepanenko, "A Sliding Mode Controller with Improved Adaptation Laws for the Upper Bounds on the Norm of Uncertainties," *Automatica* 34, pp. 1657 – 1661, 1998.

[25] H. H. Choi, "A New Method for Variable Structure Control System Design: A Linear Matrix Inequality Approach," *Automatica* 33, pp. 2089 – 2092, 1997.

[26] C. Edwards, "A practical method for the design of sliding mode controllers using linear matrix inequality," *Automatica* 40, pp. 1761 – 1769, 2004.

Abdul Rashid Husain received the B.Sc. degree in electrical and electronic engineering from The Ohio State University, Columbus, Ohio, U.S.A, in 1997, and the M.Sc. degrees in mechatonics from University of Newcastle Upon Tyne, U.K., in 2003. Before joining Universiti Teknologi Malaysia, he worked as an engineer in semiconductor industry for several years. Currently he is pursuing his PhD degree in mechatonics and control engineering and his research interest is modeling and nonlinear control of dynamic system specifically the application of Sliding Mode Control (SMC) theory for Active Magnetic bearing system.

Mohamad Noh Ahmad received the B.Sc. degree in Electrical Engineering from Universiti Teknologi Malaysia in 1986, the M.Sc. degree in Control Engineering from University of Sheffield, U.K. in 1988, and Ph.D. degree in Robotics from Universiti Teknologi Malaysia in 2003. Currently he is Associate Professor and Head of Department of the Department of Mechatronics and Robotics, Faculty of Electrical Engineering, Universiti Teknologi Malaysia. Since joining Universiti Teknologi Malaysia, his primary responsibilities include research and teaching in Robotics and Control Engineering. His researches involve among others modeling and control of numerous plants such as Active Magnetic Bearing System, Balancing Robot, and Direct-Drive Robot Manipulator.

Abdul Halim Mohamed Yatim received the B.Sc. degree in electrical and electronic engineering from Portsmouth Polytechnic, Portsmouth, U.K., in 1981, and the M.Sc. and Ph.D. degrees in power electronics from Bradford University, Bradford, U.K., in 1984 and 1990, respectively. Since 1982, he has been a member of the faculty at the Universiti Teknologi Malaysia, Johor, Malaysia, where he currently is a Professor and Deputy Dean of the Faculty. He has been involved in several research projects in the areas of power electronic applications and drives. He was a Commonwealth Fellow during 1994–1995 at Heriot-Watt University, Edinburgh, U.K., and a Visiting Scholar at the Virginia Power Electronics Center, Virginia Polytechnic Institute and State University, Blacksburg, in 1993. Dr. Yatim is a Corporate Member of the Institution of Engineers Malaysia. He is a Registered Professional Engineer with the Malaysian Board of Engineers. He currently holds the Interim Chapter Chair of the Malaysian Section of the IEEE Industrial Electronics/Industry Applications/Power Electronics Joint Societies.